

The 2023 Litli-Hrútur eruption of the Fagradalsfjall Fires, SW-Iceland: Insights from trace element compositions of olivine

Lukáš Krmíček^{1,2,3,*}, Valentin R. Troll⁴, Thor Thordarson⁵, Marek Brabec¹, William M. Moreland⁵, Adam Maťo⁶

¹Brno University of Technology, Faculty of Civil Engineering, Institute of Geotechnics, Veveří 95, CZ-602 00 Brno, Czech Republic

²Institute of Geology of the Czech Academy of Sciences, Rozvojová 269, CZ-165 02 Prague 6, Czech Republic

³BIC Brno, Technology Innovation Transfer Chamber, Purkyňova 648/125, CZ-612 00, Brno, Czech Republic

⁴Department of Earth Sciences, Section for Natural Resources & Sustainable Development, Uppsala University, Villavägen 16, S-752 36 Uppsala, Sweden

⁵Faculty of Earth Sciences, University of Iceland, Sturlugata 7, IS-102 Reykjavík, Iceland

⁶Department of Geological Sciences, Faculty of Science, Masaryk University, Kotlářská 2, CZ-611 37 Brno, Czech Republic

Abstract

This study provides data on the trace element composition of olivine from olivine tholeiitic basalts sampled during the July–August 2023 Litli-Hrútur eruption of the Fagradalsfjall Fires in the Reykjanes Volcanic Belt. Chemistry of the Litli-Hrútur olivine is characteristic for volcanic olivine crystals that represent products of magmatic crystallisation. The investigated olivine megacrysts show forsterite (Fo) content in the range of 81 (rims) to 85 (cores) mole percent [defined as $Fo = Mg/(Mg + Fe)$]. Olivine Ni concentrations (1540–1840 ppm) correlate positively with the Fo contents. In addition, Ca contents show a range from 1890 to 2460 ppm at relatively low Ti concentrations. Olivine from the Litli-Hrútur samples shows an equilibrium with peridotitic mantle melts, yet the data show that the 2023 Litli-Hrútur and the 2022 Meradalir olivine populations crystallised from compositionally more evolved magma batches than olivine crystals from the 2021 Geldingadalir eruption of the Fagradalsfjall Fires. These results imply that magmatic differentiation has taken place between the initial 2021 events and the subsequent 2022 and 2023 eruptions as a result of crystal–liquid fractionation, shifting the overall magma chemistry towards more evolved compositions with time. This implies that fractional crystallisation in sub-alkaline magma reservoirs operates on the scale of years, which is a fundamental advance in our understanding of these common magmatic systems.

DOI: 10.5817/CPR2023-2-20

Received November 27, 2023, accepted January 18, 2024.

*Corresponding author: L. Krmíček <lukas.krmicek@gmail.com>

Acknowledgements: This research was financially supported by the RVO 67985831 project of the Institute of Geology of the Czech Academy of Sciences (to LK), by the grant No. FAST-S-23-8272 at Brno University of Technology (to LK and MB), and the EXPRO 2019 project of the Czech Science Foundation (No. 19-29124X) to LK. Michaela Vašínová Galiová and Martina Machalová are thanked for technical support during data acquisition. TT and WMM acknowledge support from the Icelandic Civil Defence and the authorities. VRT acknowledges funding from the Swedish Research Council and from the Uppsala University, and the authors thank the editor-in-chief, Prof. M. Barták, for his kind invitation to submit this report as well as for his excellent editorial handling. The manuscript benefited from helpful comments by Prof. S. Altunkaynak and one anonymous reviewer.

Key words: olivine, Reykjanes Peninsula, Litli-Hrútur lava, peridotitic mantle, LA-ICP-MS

Introduction

Over the past ca. 4000 years, three 300–400 years-long eruption intervals occurred along the Reykjanes Peninsula with a repose time of 800 to 1000 years between them. These eruption intervals included the activation of four of the five volcanic systems on the peninsula, *i.e.*, the Reykjanes, Svartsengi, Krýsuvík, and the Brennisteinsfjöll magmatic systems (*e.g.*, Sæmundsson *et al.* 2020, Caracciolo *et al.* 2023, Fig. 1A). Recently, in 2021, 2022 and summer 2023, three eruptions occurred in the Fagradalsfjall volcanic lineament – the only lineament that remained inactive during the past eruption interval. Moreover, a fissure eruption began on the Sundhnúksgígar crater row (Svartsengi systems) on December 18th, 2023, with considerable force in the first hours, but lasted only three days. In the geological past, the Fagradalsfjall volcanic system has been active together with the other volcanic systems on a trans-tensional structure referred to as the Reykjanes Volcanic Belt, which links the Western Volcanic Zone to the east to the Reykjanes Ridge in the west (*e.g.*, Peate *et al.* 2009, Sæmundsson *et al.* 2020, Bindeman *et al.* 2022). It appears that we

are currently at the very beginning of a new and extended eruption interval, whereby individual lineaments of the Reykjanes Volcanic Belt may become reactivated.

In basaltic magmas from the Reykjanes Volcanic Belt, olivine is typically the first silicate mineral to crystallise. Hence, olivine provides an excellent record to help deciphering the composition of mafic parental magma from which the olivines grew, and obtain information about the composition of the mantle source (*e.g.*, Thomson and Maclennan 2013, Demouchy and Alard 2021, Krmíček *et al.* 2022, Wang *et al.* 2022, Caracciolo *et al.* 2023).

The aim of this paper is to present our preliminary data on the trace element composition of olivine from the lavas erupted in July 2023 from the vent system near Litli Hrútur, located about 3 to 4.5 km northeast of the eruption sites of the 2021 Geldingadalir and 2022 Meradalir eruptions. These data provide a first order assessment of magma origin and connection of the 2023 eruption products to the larger Fagradalsfjall magma system that reawakened in 2021.

The 2023 Litli-Hrútur eruption

On Monday, July 10th, 2023, a new basaltic eruption of the Fagradalsfjall Fires started on Reykjanes Peninsula. The eruption occurred eleven months after the end of the eruption in the more southern Meradalir valley. However, approximately eleven months also separated the end of the Meradalir eruption from the end of volcanic activity in the neighbouring Geldingadalir valley in the previous year (2021), and all three eruptions took place

within the Fagradalsfjall volcanic system (Fig. 1B).

The new eruption occurred close to the Litli-Hrútur hill (312 m a.s.l.), located approximately 40 km southwest of Reykjavík and ca. 20 km from Keflavík International Airport. The eruption was preceded by an earthquake swarm caused by a magmatic intrusion 3 km north-east of the location of the 2022 Meradalir eruption.

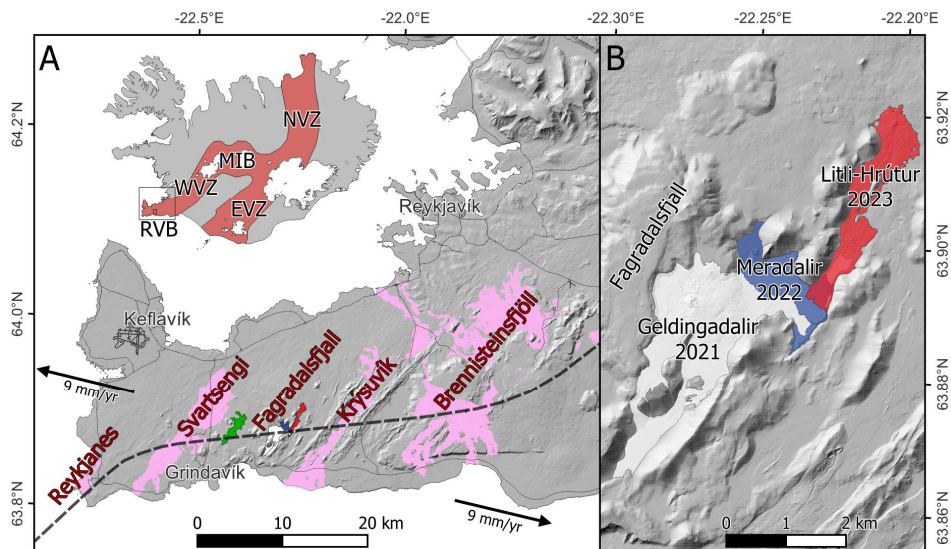


Fig. 1. Location of the studied area: A – position of the Fagradalsfjall volcanic system within the other systems (Reykjanes, Svartsengi, Krýsuvík, Brennisteinsfjöll) of the Reykjanes Volcanic Belt, the range of lava flows from the December 2023 eruption in the Sundhnúkgígur crater row is marked in green, B – detailed lava fields of the 2021 Geldingadalir, 2022 Meradalir and 2023 Litli-Hrútur eruptions. Abbreviations: RVB (Reykjanes Volcanic Belt), WVZ (Western Volcanic Zone), MIB (Mid-Iceland Belt), NVZ (Northern Volcanic Zone), EVZ (Eastern Volcanic Zone).

The 2023 Litli-Hrútur eruption began with an impressive curtain of lava fountaining along a set of en-echelon fissure segments. The main fissure, oriented in the northeast–southwest direction, originally measured approximately 200 m in length. At the start, the magma discharge was $40 \text{ m}^3 \cdot \text{s}^{-1}$ and stabilised at a value of around $10 \text{ m}^3 \cdot \text{s}^{-1}$ (dense rock equivalent) in the first days, to ultimately focus on a single location where the main spatter cone was later built (e.g., [1], [2]). The lava along the entire length of the fissure caused widespread (moss-)fires in the surrounding dry vegetation and compared to the previous eruptions of 2021 and 2022, burning vegetation in the vicinity of Litli-Hrútur affected a relatively larger area (Krmíček 2023). Together with volcanic gases (CO_2 , SO_2 , H_2S), a poisonous cloud formed around the volcano, which largely drifted southwest over the Atlantic Ocean

in the following days (Fig. 2). The rapid onset of the eruption, accompanied by extreme air pollution, led the Icelandic authorities to decide to reduce access to the vicinity of the newly formed Litli-Hrútur cinder cone (Fig. 3A) on several occasions during the eruptive events.

A dramatic event during the eruption occurred on the night of July 18th to 19th. The western side of the cinder cone, which was up to 30 m in height at the time, collapsed outward (e.g., [1], [2], Krmíček 2023, Fig. 3B). A larger volume of lava that had accumulated inside the crater spilled into the surroundings, creating a larger lava pond on the western side of the main vent system and accelerated lava outpourings towards the south into the Meradalir area for some time. Ultimately, lavas flowing south met the lavas of the 2021 Geldingadalir and 2022 Meradalir eruptions and partly covered these in the

eastern section of the Meradalir valley system (Fig. 3C). After this event, magma discharge from the Litli-Hrútur vent reduced steadily, and a smaller cinder cone

formed inside the original cone a few days before the end of the eruption. The eruption was declared over on Saturday, August 5th, less than a month after it began.



Fig. 2. The 2023 Litli-Hrútur eruption began with a Hawaiian-style lava fountaining along the volcanic fissure. In the first days of the eruption, a poisonous cloud formed around the fissure and was drifted southwest over the Atlantic Ocean. Image contains modified Copernicus Sentinel data (2023), processed by ESA, CC BY-SA 3.0 IGO (https://www.esa.int/ESA_Multimedia/Terms_and_Conditions).

Fig. 3. ► Field photos from the Litli-Hrútur area: A – a view of the spatter cone as it formed above the fissure eight days after the eruption began, B – a photo from July 19 shows a view of the lava pond on the western side of the cone after the collapse of its western wall, C – broken crust of the ropy lava from the 2021 Geldingalir eruption in Meradalir being covered by the 2023 Litli-Hrútur lava flow.



Sampling the Litli-Hrútur eruption

The main task of our field volcanology team was collecting georeferenced samples of solid and liquid lava as well as pyroclastic material ejected in the vicinity of the main cinder cone (Fig. 4A). Pyroclastic products were collected, similarly to the previous two eruptions, from free-lying, highly vesicular and occasionally reticulite-like tephra. In addition, it was possible to come across various morphological forms of volcanic bombs, the size of which varied from several cm to tens of centimetres. Around the cone, most of the ejected material hit the ground in a sufficiently hot

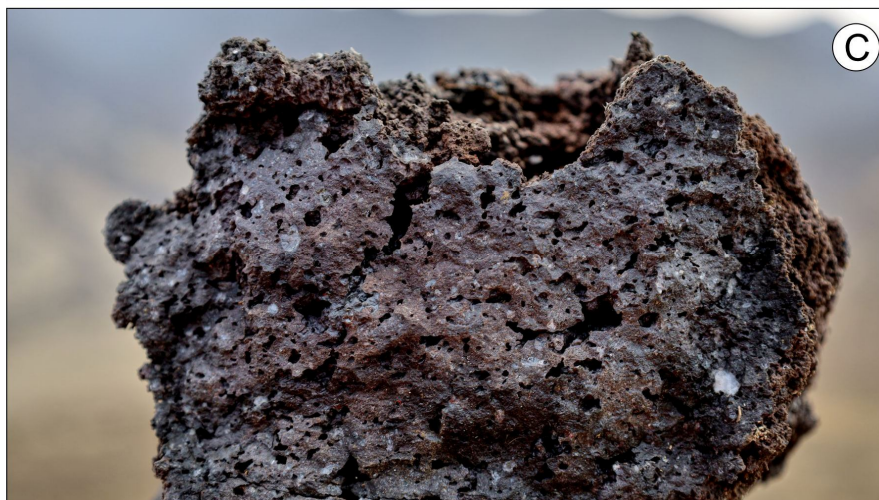
and plastic state to form characteristically flattened (cow-pie) bombs. A morphologically different type of bomb was collected at a greater distance from the crater. There, the rapidly solidifying basalt lava took on a more aerodynamic shape during the longer flight, and was twisted to spindle shapes due to the rotation during aerial transport. Feldspar-phyric lava investigated in this study was collected during the active phase of the Litli-Hrútur eruption on July 17th from the northernmost tip of the initial volcanic fissure (Fig. 4B, C).

Analytical methods

The collected material was cut with a diamond saw, and then a paired set of polished sections (30 μm and 150 μm thick) was made from the rock slices mounted on glass slides. The thinner polished sections were examined using conventional optical microscopy to evaluate the presence and shapes of individual olivine crystals. The composition of selected olivine grains was analysed in the thicker polished sections using an electron probe micro-analyser (EMPA) and subsequently by laser ablation inductively coupled plasma mass spectrometry (LA-ICP-MS). The LA-ICP-MS facility consisted of quadrupole-based ICP-MS (Agilent 7900) connected to the ArF* excimer laser ablation system Analyte

Excite+ (Teledyne CETAC Technologies) hosted at the Brno University of Technology. The laser ablation system emits a laser beam at a wavelength of 193 nm, and is equipped with 2-vol Cell HelEx II. The ablated material was carried by He flow (0.5 and 0.3 $\text{l} \cdot \text{min}^{-1}$) and mixed with Ar ($\sim 1 \text{ l} \cdot \text{min}^{-1}$) prior to entering the ICP mass spectrometer. The sample surface was ablated for 60 s per spot using a laser beam diameter of 50 μm with the fluence of 3 $\text{J} \cdot \text{cm}^{-2}$, 10 Hz repetition rate and 60 s washout time. The monitored isotopes are as follows: ${}^7\text{Li}^+$, ${}^{11}\text{B}^+$, ${}^{23}\text{Na}^+$, ${}^{27}\text{Al}^+$, ${}^{29}\text{Si}^+$, ${}^{31}\text{P}^+$, ${}^{44}\text{Ca}^+$, ${}^{45}\text{Sc}^+$, ${}^{47}\text{Ti}^+$, ${}^{51}\text{V}^+$, ${}^{52}\text{Cr}^+$, ${}^{55}\text{Mn}^+$, ${}^{60}\text{Ni}^+$, ${}^{63}\text{Cu}^+$, ${}^{66}\text{Zn}^+$, ${}^{69}\text{Ga}^+$, ${}^{73}\text{Ge}^+$, ${}^{89}\text{Y}^+$, ${}^{90}\text{Zr}^+$, ${}^{93}\text{Nb}^+$, ${}^{118}\text{Sn}^+$, ${}^{181}\text{Ta}^+$ and ${}^{208}\text{Pb}^+$.

Fig. 4. ► Litli-Hrútur volcano sampling: A – the collection of liquid lava was done in part in collaboration with scientists from the University of Buffalo, B – investigated lava from the northernmost tip of the initial volcanic fissure indicated by red dashed line, C – lava sample containing conspicuous plagioclase phenocrysts.



The ICP-MS was calibrated using SRM NIST 612 (Standard Reference Material of National Institute of Standards and Technology) with respect to the sensitivity and minimum doubly charged ions ($\text{Ce}^{2+}/\text{Ce}^+ < 5\%$), oxide formation ($^{248}\text{ThO}^+/^{232}\text{Th}^+ < 0.3\%$) and mass response $^{238}\text{U}^+/^{232}\text{Th}^+ \sim 1$. The potential interferences were minimised via a collision cell ($\text{He } 1 \text{ ml} \cdot \text{min}^{-1}$). The elemental contents were quantified using artificial glass standards SRM NIST 610 and 612,

and Si (determined by EPMA) as the internal reference element after baseline correction and integration of the peak area using HDIP (HDF-based Image Processing) software (Teledyne CETAC Technologies, Omaha, Nebraska, USA). The elemental content was also checked via ablation of MongOL Sh11–2 olivine standard (Batanova *et al.* 2019) as unknown material. Representative trace element olivine data are listed along with the average detection limits in Table 1.

	LHL1	LHL2	LHL3	LHL4	LHL5	LHL6	LHL7	LHL8	LHL9	LOD	LOQ
Al	203	276	543	691	540	301	245	231	259	2.30	7.65
P	172	366	333	145	209	202	334	261	416	37.4	125
Ca	2049	1975	2456	2396	2327	2073	1893	1980	1902	95.8	319
Sc	10.9	12.4	12.3	11.2	10.5	11.5	11.3	11.0	12.2	0.39	1.30
Ti	39.3	52.2	76.3	84.9	69.7	58.4	55.9	50.7	58.9	1.01	3.38
V	7.02	8.11	9.09	9.30	8.46	8.73	8.71	8.03	9.18	0.12	0.41
Cr	286	321	334	297	293	349	406	349	422	1.04	3.48
Mn	1619	1547	1561	1681	1651	1849	1545	1613	1546	0.77	2.57
Ni	1561	1788	1641	1664	1540	1742	1841	1791	1810	0.71	2.38
Cu	4.50	4.75	5.83	6.14	4.97	7.53	4.83	4.23	4.78	0.30	0.99
Zn	91.3	91.8	98.6	102	96.3	107	89.9	94.6	88.8	0.61	2.03
Ga	0.12	0.20	0.24	0.26	0.20	0.18	0.15	0.13	0.17	0.04	0.12
Y	1.01	0.12	0.16	0.20	0.16	0.14	1.18	0.08	0.08	0.01	0.05
Zr	<i>0.03</i>	<i>0.04</i>	0.27	0.42	0.27	0.30	0.07	<i>0.02</i>	<i>0.03</i>	0.01	0.05

Table 1. Representative trace element compositions (in ppm) of Litli-Hrútur olivine. Values below limit of quantification are given in italics. The contents of Li, B, Na, Ge, Nb, Sn, Ta and Pb are below their detection limits. The possible effect of polyatomic interference $^{29}\text{Si}^{16}\text{O}$ on mass-45 was negligible for the given concentrations of Sc. *Abbreviations:* LOD = limit of detection, LOQ = limit of quantification.

Results

The lava samples from Litli-Hrútur consist of olivine tholeiite basalts characterised by abundant plagioclase, minor olivine, and clinopyroxene megacrysts surrounded by a finely crystalline to glassy groundmass (Fig. 5). Olivine megacrysts are present as subhedral to euhedral prisms with variable MgO contents [Fo_{85-81} , where $\text{Fo} = \text{Mg}/(\text{Mg}+\text{Fe}) \text{ mol}\%$]. Nickel concentrations correlate positively with Fo con-

centration and range between 1540 and 1840 ppm. Olivine also shows Mn concentrations ranging from 1545 to 1850 ppm, whereas Ca contents range from 1890 to 2460 ppm at relatively low Ti (40–85 ppm). Aluminium (200–690 ppm), Zn (90–110 ppm) and Ga (up to 0.26 ppm) concentrations are comparable to the previously published data for Icelandic olivine (*e.g.*, Rasmussen *et al.* 2020, Krmíček *et al.* 2022).

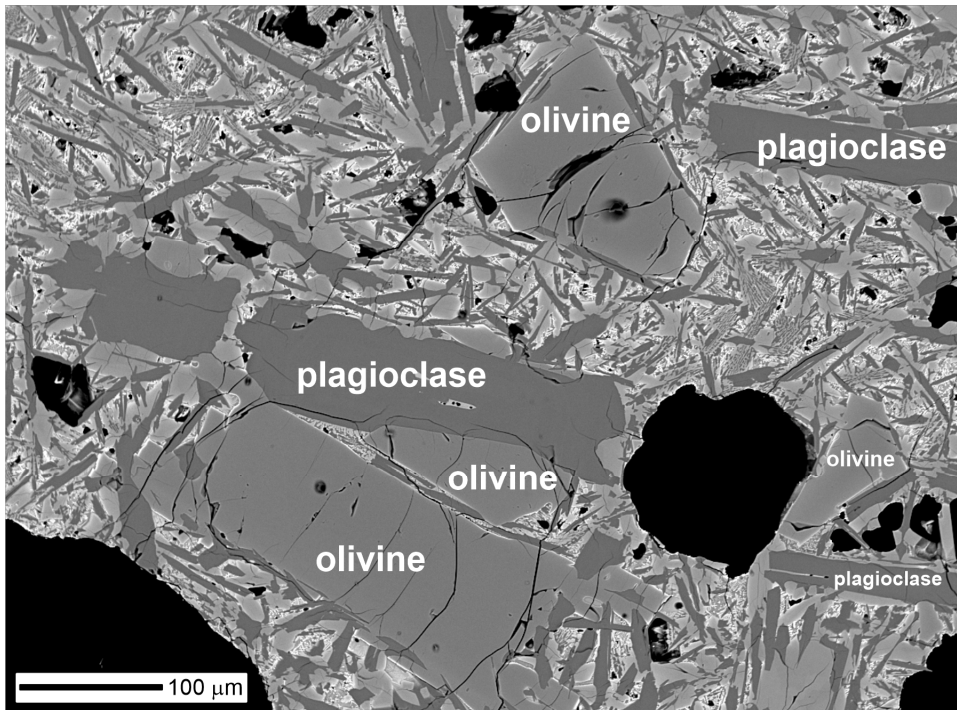


Fig. 5. Litli-Hrútur lava samples are characterised by plagioclase and olivine (\pm clinopyroxene) phenocrysts and microphenocrysts sitting in a finely crystalline to glassy groundmass (back-scattered electron image).

Discussion

A specific signature of volcanic olivine

According to Foley et al. (2013), mantle-derived (xenocrystic) olivine can be distinguished from volcanic olivine by distinctly lower concentrations of Ca (<700 ppm) and Ti (<70 ppm). Hence, trace element compositions of olivine from Litli-Hrútur provide evidence that all investigated megacrysts correspond to high-Ca olivine of volcanic origin, rather than crystal cargo from disintegrated mantle peridotite or pyroxenite, or similar upper mantle lithologies. On the other hand, the investigated olivine is also characterised by relatively low Ti contents, typically found in mantle olivine. Similar compositional features were also observed in olivine from the

previous eruptions of the Fagradalsfjall Fires (Krmíček et al. 2022). Volcanic olivine from the 2022 Meradalir and 2023 Litli-Hrútur eruptions, however, must represent the product of crystallisation from a magma that was more compositionally evolved than the magma producing olivine during the 2021 Geldingadalir eruption. The 2021 olivine crystals are characterised by higher MgO contents (up to Fo₉₀; Halldórsson et al. 2022), and thus contrasts the Fo range from 85 down to 81 recorded in our 2023 olivine samples.

Howarth and Harris (2017) proposed the use of Mn/Zn ratios in olivine to distinguish between pyroxenite and peridotite

as the predominant source lithology. Olivines derived from a pyroxenite source are characterised by low Mn/Zn ratios (<14), whereas those from peridotitic sources have usually higher ratios (>14). Based on the current data from this study, composition of olivine from the Litli-Hrútur samples, together with olivine from previous eruptions of the Fagradalsfjall Fires (Krmíček *et al.* 2022) and olivine from older lavas of the Reykjanes Volcanic

Belt (Rasmussen *et al.* 2020) fall within the high Mn/Zn ratio domain, indicating melting of a dominantly peridotite mantle source (Fig. 6). In contrast, trace element composition of olivine from the southeast propagating Eastern Volcanic Zone (South Iceland Volcanic Zone *sensu* Rasmussen *et al.* 2020) fall mostly within the field for olivine in equilibrium with ('plume-enriched') pyroxenite melts (*cf.* Krmíček *et al.* 2022).

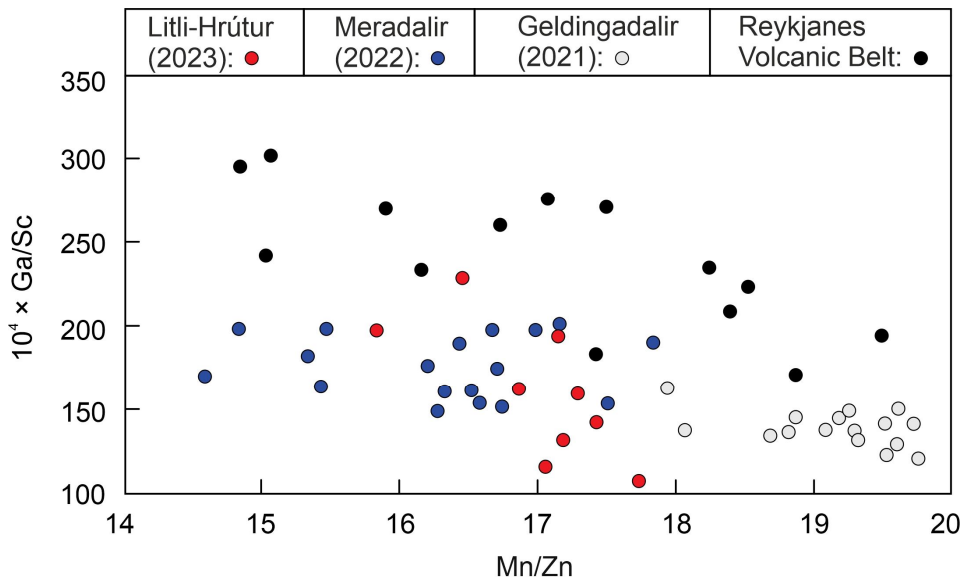


Fig. 6. Olivine compositional variations in Litli-Hrútur samples in Ga/Sc *versus* Mn/Zn diagram. Position of analytical spots for olivine from the Meradalir and Geldingadalir lavas is according to Krmíček *et al.* (2022). Olivine composition for the Reykjanes Volcanic Belt is taken from Rasmussen *et al.* (2020), who also marked this zone as the Western Volcanic Zone.

Litli-Hrútur in the context of recent eruptions of the Fagradalsfjall Fires

From the very start of the eruption, the 2023 Litli-Hrútur eruption showed similarities with the 2022 eruption in Meradalir. The life cycle of both eruptions was relatively short, lasting only a few weeks and less than a month in both cases. In both cases, the initial rapid onset of the eruption was replaced in the following days and weeks by a steady decrease in lava outflow

rate and also similarly, the eruptions began to concentrate in one main vent system soon after the fissure eruptions commenced. Moreover, the common feldsparphyric lavas from the very beginning of both eruptions points to the fact that the source(s) of 2022 and 2023 eruptions developed at crustal conditions for some time before the eruption started. This is because

feldspar crystallisation requires crustal formation pressures and needs some time (months to years for H₂O-bearing basaltic melts; *see* Arzilli et al. 2015 and references therein) to grow to megascopic dimensions. However, there are several differences in the case of the six-month lasting 2021 event. There, a different eruption dynamics was observed, comprising the opening of successive volcanic fissures with a total of six new volcanic craters or vent systems developing successively throughout the Geldingadalir valley (*e.g.*, Barsotti et al. 2023). This indicates the presence of a more complex plumbing system located deep under the volcano, and components from different sources located near the Moho discontinuity were thus mixed during the eruption in the Geldingadalir valley (*see* also Radu et al. 2023 and references therein). In addition, changes from feldspar poorer and olivine richer lava compositions to olivine poor and feld-

spar rich compositions were observed during the 2021 Geldingadalir eruption (*e.g.*, Bindeman et al. 2022, Halldórsson et al. 2022), implying different source regions to have contributed at different stages of the 2021 eruption.

Adding to these observations, the chemical composition of olivine, *e.g.*, the genetically important element nickel, shows that (volcanic) olivine from the 2021 Geldingadalir eruption records values comparable to values typical of the mantle. This contrasts the concentrations of nickel in olivine from the 2023 Litli-Hrútur and 2022 Meradalir eruptions, which are noticeably lower (generally below 2000 ppm, Fig. 7). Moreover, a broad trend towards gradual Sc enrichment of olivine, showing olivine from Litli-Hrútur lavas being the most Sc enriched, is observed amongst the eruptions of the Fagradalsfjall Fires (Fig. 7).

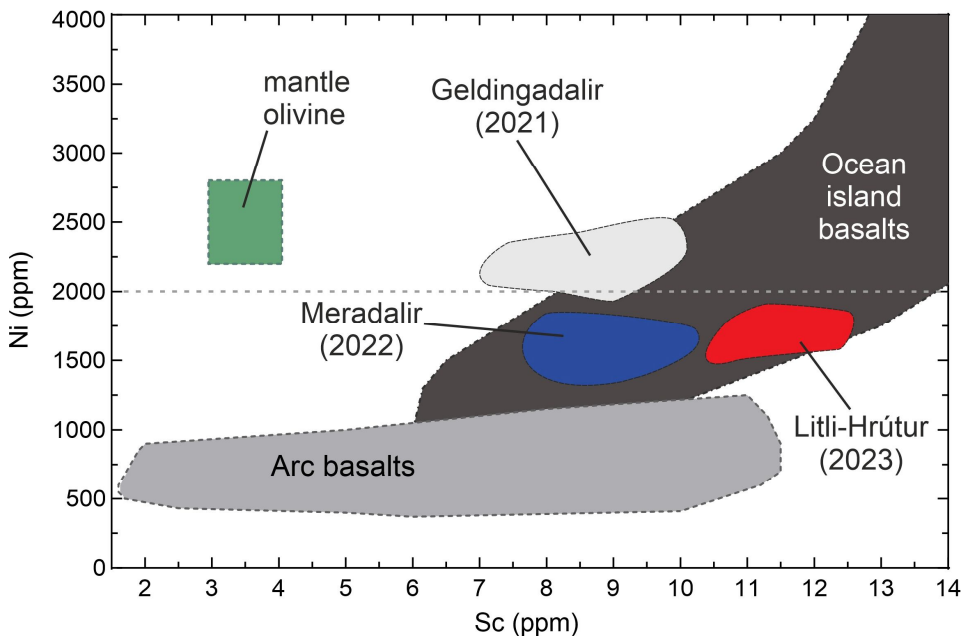


Fig. 7. The position of the studied samples in Ni *versus* Sc diagram supplemented by the data for olivine from the Meradalir (Krmíček et al. 2022) and Geldingadalir (unpublished data) initial lavas. Fields for the olivine composition of oceanic island basalts, arc basalts and mantle olivine are plotted according to Foley et al. (2013).

It is known that partial melting of fertile spinel peridotite could produce Sc-rich primary melts, whereas melts derived from garnet peridotite are generally characterised by low Sc concentrations (Wang *et al.* 2021). Thus, observed Sc variations might be controlled by different abundance of garnet *versus* spinel in the peridotite mantle source both on regional (Reykjanes Volcanic Belt *versus* Eastern Volcanic Zone; Krmíček *et al.* 2022) and local scales. The collected data for the Fagradalsfjall volcanic system may point to a decreasing depth of partial mantle melting from 2021

Geldingadalir towards 2023 Litli-Hrútur eruptions.

Based on initial results of the characterisation of rock samples collected on the 19th of December 2023 during the eruption at Sundhnúksíggar crater row, the lava is more evolved (lower MgO) than the recent eruptions of the Fagradalsfjall Fires, suggesting that modifications of parental melts following crustal storage is even more important than in recent Fagradalsfjall eruptions (*cf.* [3]). Study of olivine composition from this eruption will be the subject of some of our future investigations.

Conclusions

Based on our results, the following main conclusions can be drawn:

(1) Trace element compositions of Litli-Hrútur olivine provide evidence that the investigated olivine crystals are high-Ca (and low-Ti) olivine of volcanic origin, rather than recycled mantle cargo.

(2) Volcanic olivines from fresh lava samples, both from the 2023 Litli-Hrútur and the 2022 Meradalir eruptions, represent the product of crystallisation from compositionally more evolved magma(s)

compared to olivine crystals from the 2021 Geldingadalir eruption.

(3) Olivine crystals from the 2023 Litli-Hrútur samples are characteristic for a source magma that formed from melting of a dominantly peridotitic mantle source.

(4) Variable but broadly increasing Sc contents may reflect decreasing depth of the partial melting of a peridotitic mantle source from the 2021 Geldingadalir towards the 2023 Litli-Hrútur eruptions.

References

- ARZILLI, F., AGOSTINI, C., LANDI, P., FORTUNATI, A., MANCINI, L. and CARROLL, M. R. (2015): Plagioclase nucleation and growth kinetics in a hydrous basaltic melt by decompression experiments. *Contributions to Mineralogy and Petrology*, 170: 55. doi: 10.1007/s00410-015-1205-9
- BARSOTTI, S., PARKS, M. M., PFEFER, M. A., ÓLADÓTTIR, B. A., BARNIE, T., TITOS, M. M., JÓNSDÓTTIR, K., PEDERSEN, G. B. M., HIARTARDÓTTIR, Á. R., STEFANSDÓTTIR, G., JÓHANSSON, T., ARASON, P., GUDMUNDSSON, M. T., ODDSSON, B., PRASTARSON, R. H., ÓFEIGSSON, B. G., VOGJÖRD, K., GEIRSSON, H., HIÖRVAR, T., VON LÖWIS, S., PETERSEN, G. N. and SIGURÐSSON, E. M. (2023): The eruption in Fagradalsfjall (2021, Iceland): How the operational monitoring and the volcanic hazard assessment contributed to its safe access. *Natural Hazards*, 116(3): 3063-3092. doi: 10.1007/s11069-022-05798-7
- BATANOVA, V. G., THOMPSON, J. M., DANYUSHEVSKY, L. V., PORTNYAGIN, M. V., GARBE-SCHÖNBERG, D., HAURI, E., KIMURA, J. I., CHANG, Q., SENDA, R., GOEMANN, K., CHAUVEL, C., CAMPILLO, S., IONOV, D. A. and SOBOLEV, A. V. (2019): New olivine reference material for in situ microanalysis. *Geostandards and Geoanalytical Research*, 43(3): 453-473. doi: 10.1111/ggr.12266

- BINDEMAN, I. N., DEEGAN, F. M., TROLL, V. R., THORDARSON, T., HÖSKULDSSON, Á., MORELAND, W. M., ZORN E. U., SHEVCHENKO, A. V. and WALTER, T. R. (2022): Diverse mantle components with invariant oxygen isotopes in the 2021 Fagradalsfjall eruption, Iceland. *Nature Communications*, 13(1): 1-12. doi: 10.1038/s41467-022-31348-7
- CARACCILO, A., BALI, E., HALLDÓRSSON, S. A., GUÐFINNSSON, G. H., KAHL, M., ÞÓRDARDÓTTIR, I., PÁLMAÐÓTTIR, G. L. and SILVESTRI, V. (2023): Magma plumbing architectures and timescales of magmatic processes during historical magmatism on the Reykjanes Peninsula, Iceland. *Earth and Planetary Science Letters*, 621: 118378. doi: 10.1016/j.epsl.2023.118378
- DEMOUCHY, S., ALARD, O. (2021): Hydrogen, trace, and ultra-trace element distribution in natural olivines. *Contributions to Mineralogy and Petrology*, 176: 1-25. doi: 10.1007/s00410-021-01778-5
- FOLEY, S. F., PRELEVIC, D., REHFELDT, T. and JACOB, D. E. (2013): Minor and trace elements in olivines as probes into early igneous and mantle melting processes. *Earth and Planetary Science Letters*, 363: 181-191. doi: 10.1016/j.epsl.2012.11.025
- HALLDÓRSSON, S. A., MARSHALL, E. W., CARACCILO, A., MATTHEWS, S., BALI, E., RASMUSSEN, M. B., RANTA, E., ROBIN, J. G., GUÐINNSSON, G. H., SIGMARSSON, O., MACLENNAN, J., JACKSON, M. G., WHITEHOUSE, M. J., JEON, H., VAN DER MEER, Q. H. A., MIBEL, G. K., KALLIOKOSKI, M. H., REPCZYNSKA, M. M., RÚNARSDÓTTIR, R. H., SIGURÐSSON, G., PFEFER, M. A., SCOTT, S. W., KJARTANSDÓTTIR, R., KLEINE, B. I., OPPENHEIMER, C., AIUPPA, A., ILYINSKAYA, E., BITETTO, M., GIUDICE, G. and STEFÁNSSON, A. (2022): Rapid shifting of a deep magmatic source at Fagradalsfjall volcano, Iceland. *Nature*, 609: 529-534. doi: 10.1038/s41586-022-04981-x
- HOWARTH, G. H., HARRIS, C. (2017): Discriminating between pyroxenite and peridotite sources for continental flood basalts (CFB) in southern Africa using olivine chemistry. *Earth and Planetary Science Letters*, 475: 143-151. doi: 10.1016/j.epsl.2017.07.043
- KRMÍČEK, L. (2023): Litli-Hrútur: The life cycle of Iceland's youngest volcano. *Vesmír*, 102: 640-643.
- KRMÍČEK, L., TROLL, V. R., GALIOVÁ, M. V., THORDARSON, T. and BRABEC, M. (2022): Trace element composition in olivine from the 2022 Meradalir eruption of the Fagradalsfjall Fires, SW-Iceland. *Czech Polar Reports*, 12(2): 222-231. doi: 10.5817/CPR2022-2-16
- PEATE, D. W., BAKER, J. A., JAKOBSSON, S. P., WRIGHT, T. E., KENT, A. J., GRASSINEAU, N. V. and SKOVGAARD, A. C. (2009): Historic magmatism on the Reykjanes Peninsula, Iceland: A snapshot of melt generation at a ridge segment. *Contributions to Mineralogy and Petrology*, 157(3): 359-382. doi: 10.1007/s00410-008-0339-4
- RADU, I. B., SKOGBY, H., TROLL, V. R., DEEGAN, F. M., GEIGER, H., MÜLLER, D. and THORDARSON, T. (2023): Water in clinopyroxene from the 2021 Geldingadalir eruption of the Fagradalsfjall Fires, SW-Iceland. *Bulletin of Volcanology*, 85(5): 31. doi: 10.1007/s00445-023-01641-4
- RASMUSSEN, M. B., HALLDÓRSSON, S. A., GIBSON, S. A. and GUÐFINNSSON, G. H. (2020): Olivine chemistry reveals compositional source heterogeneities within a tilted mantle plume beneath Iceland. *Earth and Planetary Science Letters*, 531: 116008. doi: 10.1016/j.epsl.2019.116008
- SÆMUNDSSON, K., SIGURGEIRSSON, M. Á. and FRÍÐLEIFSSON, G. Ó. (2020): Geology and structure of the Reykjanes volcanic system, Iceland. *Journal of Volcanology and Geothermal Research*, 391: 106501. doi: 10.1016/j.jvolgeores.2018.11.022
- THOMSON A. R., MACLENNAN, J. (2013): The distribution of olivine compositions in Icelandic basalts and picrites. *Journal of Petrology*, 54(4): 745-768. doi: 10.1093/petrology/egs083
- WANG, Z., LI, M. Y. H., LIU, Z. R. R. and ZHOU, M. F. (2021): Scandium: Ore deposits, the pivotal role of magmatic enrichment and future exploration. *Ore Geology Reviews*, 128: 103906. doi: 10.1016/j.oregeorev.2020.103906
- WANG, C., ZHANG, Z., GIULIANI, A., DEMOUCY, S., THORAVAL, C., KRMÍČEK, L., BO, H., ZHANG, W. and XIA, X. (2022): Hydrogen concentrations and He isotopes in olivine from ultramafic lamprophyres provide new constraints on a wet Tarim Plume and Earth's deep water cycle. *Journal of Geophysical Research: Solid Earth*, 127(12): e2022JB024961. doi: 10.1029/2022JB024961

Web sources / Other sources

- [1] Icelandic Meteorological Office.
<https://en.vedur.is/about-imo/news/earthquake-activity-in-fagradalsfjall-area>
- [2] Rannsóknareining í eldfjallafræði og náttúruvá, Háskóli Íslands.
https://www.facebook.com/Natturuva?locale=ms_MY
- [3] Institute of Earth Sciences, University of Iceland.
<https://earthice.hi.is/first-results-characterisation-rock-samples-collected-eruption-sundhnuksgigar-crater-row>